I&EC research
Industrial & Engineering Chemistry Research

pubs.acs.org/IECR Article

Catalytic Hydroxyalkylation/Alkylation of 2-Methylfuran with Butanal to Form a Biodiesel Precursor Using Acidic Ion-Exchange Resins

Eliana Ramírez,* Rodrigo Soto, Roger Bringué, Montserrat Iborra, and Javier Tejero

Cite This: https://dx.doi.org/10.1021/acs.iecr.0c04308 Read Online

ACCESS | Metrics & More | Article Recommendations

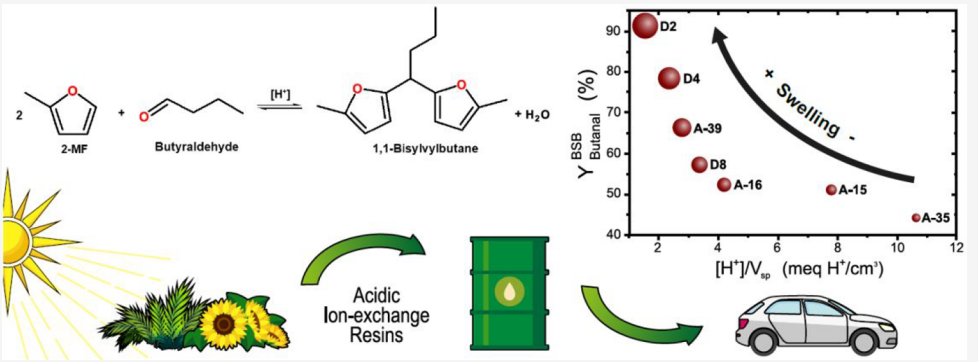

ABSTRACT: The catalytic hydroxyalkylation/alkylation of 2-methylfuran (2MF) with butanal has been investigated over several acidic ion-exchange resins within the temperature range 50−90 °C and at a stoichiometric reactant molar ratio of 2MF/butanal (2:1). Butanal conversion increases with temperature and also the formation of undesired 2-methylfuran oligomers, leading to a decrease in yield of the target product. The highest butanal conversion (90%) is achieved at 50 °C over Dowex 50Wx2 with a negligible formation of 2-methylfuran oligomers. The observed catalytic activity and final yield of the target product have been rationalized on the basis of morphological properties of resins and their dynamic behavior within the present reaction medium. The findings reveal that gel-type resins are more active and render higher product yields than their macroreticular congeners due to the enhanced accessibility to acid centers because of their improved ability to swell throughout the reaction. Macroreticular resins with a low cross-linking degree, e.g., Amberlyst39, also produce interesting catalytic results. The stability of the most promising catalyst has been evaluated after three reaction cycles, and the full reusability outcome speaks for its appropriateness as a potential catalyst for the studied process.

1. INTRODUCTION

The continuous exploitation of irreplaceable oil reserves and the ensuing increase of its derived environmental effects has generated the need for green alternative fuels, platforms, and fine chemicals. From this scenario, biomass emerges as the only renewable, widespread, abundant, and cheap source of carbon-based materials that can be considered a plausible substitute for petroleum.[1] The hydrolysis of biomass is a selective process of depolymerization by dissociation of energy-neutral C−O bonds that yields C5 and C6 monosaccharides, e.g., glucose, fructose, and xylose, which preserve the energy-profitable C−H and C−C bonds.[2,3] Further processing of these hydrocarbons renders a wide array of platform chemicals, e.g., levulinic acid,[4,5] 5-hydroxymethylfurfural, furfural, and 2-methylfuran,[6] which can be used for the synthesis of highly valuable components for transportation fuels and the production of fine chemicals.[7] Among them, 2-methylfuran (2MF, also known as sylvan)[8] obtained from furfural has recently attracted interests for biofuel production due to its versatility to direct blending with gasoline[9] and diesel[10] and to synthesize high-density biofuel.[11] For instance, the hydroxyalkylation/alkylation (HAA) of sylvan with *n*-butanal produces 1,1-bisylvylbutane (BSB), which can be transformed into 6-propyl undecane by a subsequent hydrodeoxygenation (HDO) step in series. Using platinum-supported carbon- or alumina-based catalysts, a mixture of C9, C12, and C14 alkanes can be obtained as an organic phase from the second reaction

Received: September 1, 2020
Revised: October 21, 2020
Accepted: November 4, 2020

Scheme 1. Hydroxyalkylation/Alkylation of Sylvan with Butyraldehyde to Produce 1,1-Bisylvylbutane (BSB)

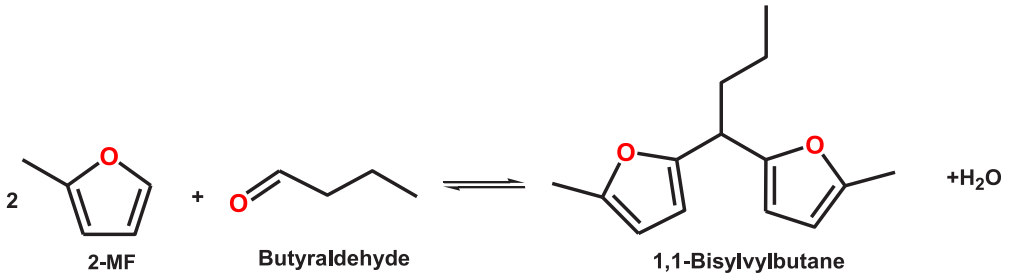

Scheme 2. Self-Condensation of 2-Methylfuran to Form Its Trimer and Tetramers

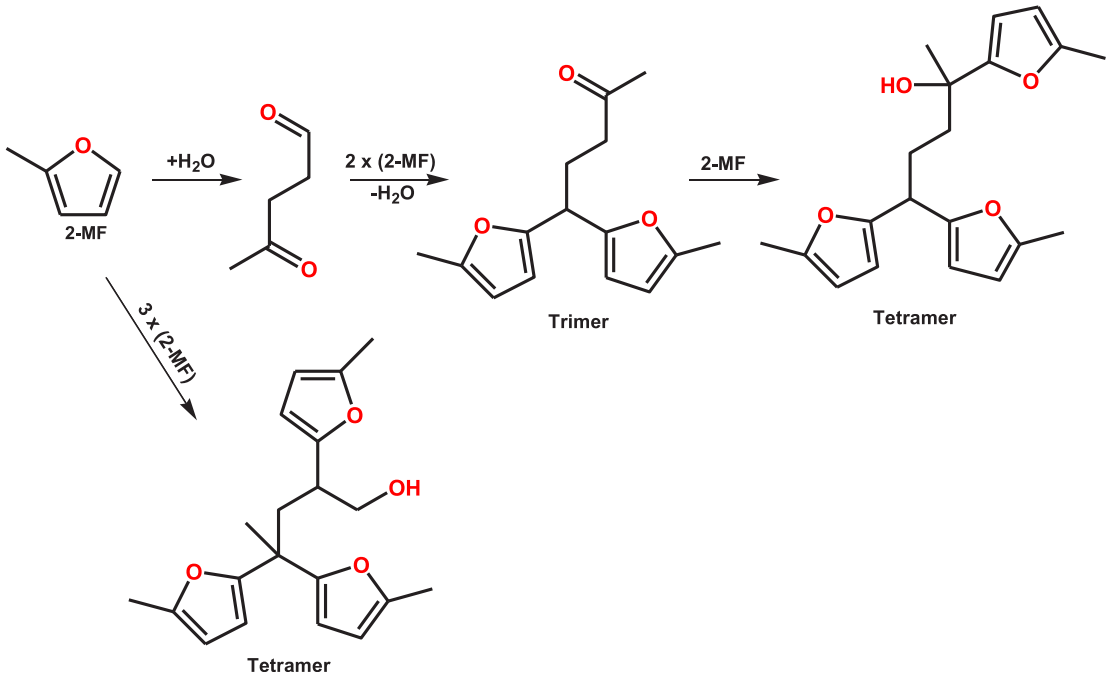

step[12] with excellent diesel fuel properties, e.g., pour point of −90 °C and cetane number of 71.[13] In the first reaction step, sylvan molecules can react with different aldehydes and ketones to give a precursor with an adequate carbon atom number that can be further hydrogenated to yield $C12^+$ oxygenated intermediate molecules. Such a pathway is illustrated in Scheme 1 using butanal as an alkylating agent. The use of butanal presents the advantage of being a bioreactant since it can be produced by partial oxidation or dehydrogenation of biobutanol obtained from the acetone-butanol-ethanol (ABE) fermentation process.[14]

During the cross-condensation of 2-methylfuran with *n*-butanal to form BSB (Scheme 1), some side reactions can also take place (Scheme 2) originated from the self-condensation of 2MF that produces a trimer (5,5-bis(5-methylfuran-2-yl) pentan-2-one or 5,5-bisylvyl-2-pentanone) and a tetramer (2,4,4-trisylvyl-2-pentanol or 2,4,4-tris(5-methylfuran-2-yl)-pentan-2-ol).[8,14,15] An implicit drawback that makes working with 2MF challenging is its ease to polymerize in the presence of acid catalysts, even under moderate acid conditions, e.g., phosphoric acid.[16] Accordingly, different types of catalysts have been tested in the hydroxyalkylation/alkylation of sylvan with carbonyl compounds,[3,8,17] aiming to control polymerization that results in a brown viscous liquid comprising tetra-, penta-, hexa-, and heptamers.

Interesting yields and conversions ranging from 60 to 100% have been reported for the HAA of sylvan with butanal (Scheme 1) over different types of catalysts such as $NbOPO_4$,[18] improved graphene oxide,[19] copper(II) triflate,[20] Sn-beta(12.5) zeolite,[21] Nafion 212,[15,22] Amberlyst15 (A15),[8,12,15,22] and Amberlyst36 (A36),[15,22] Dowex 50Wx2,[8,12] protonated titanate nanotubes,[23] KCC-1APSO$_3$H,[15] and acidic carbon catalysts (60LS40PS350H$^+$).[24] Further details on the experimental conditions and results reported are provided in section 3.1 for a proper comparison.

The state of the art reveals that the range of reaction temperatures for the HAA of sylvan is fully compatible with the operating temperatures of standard ion-exchange resins (<150 °C), whose active sites can catalyze the reaction in Scheme 1.[25] However, the number of studies for this reaction over acidic ion-exchange resins is scarce and limited to only a few resins, being Amberlyst (A15) the most frequently used. Interestingly, A15 is of macroreticular nature and, hence, of questionable application for systems in which water is a reaction product and that involve products of relatively big molecular volume, for which gel-type resins should be more suitable.[26] Ion-exchange resins are environmentally friendly catalysts because of their nontoxicity, noncorrosiveness, and cost-effective recyclability. They can be synthesized in a wide variety of

https://dx.doi.org/10.1021/acs.iecr.0c04308
Ind. Eng. Chem. Res. XXXX, XXX, XXX−XXX

tunable properties, e.g., acid capacity, pore diameter, and cross-linking degree, making them excellent catalysts to investigate the relations between catalytic activity and catalysts morphology for different applications.

The present work aims to shed light in this regard by the evaluation of several ion-exchange resins of different characteristics for the HAA of sylvan with butanal. The main objective is to identify the optimum catalyst properties and experimental conditions that maximize BSB production and minimize the extent of side reactions. Therefore, special emphasis is devoted to a comprehensive analysis that allows for rationalizing the relations between catalysts' morphological properties and the reported catalytic activity. In addition, the stability of the best catalyst selected is evaluated by several reaction cycles in the most promising conditions.

2. EXPERIMENTAL SECTION

2.1. Chemicals. Butyraldehyde (butanal, 99% dry) and 2-methylfuran (sylvan, 2MF, 99%), both supplied by Sigma-Aldrich, were used as reactants and standards without further purification. As BSB is not a commercial product, its standard for calibration was obtained from the organic phase of preliminary experiments. After distillation, the purity of BSB was 98% GC. Nitrogen (99.999% GC) and helium (99.998% GC) supplied by Air Liquid were used to pressurize the system and for the chromatographic analyses. For catalyst reusability tests, dry methanol (0.005 wt % of water, Panreac AppliChem), water (Milli-Q, Millipore Corp.), and hydrogen peroxide (30% w/v, Panreac AppliChem) were used as reagents.

2.2. Catalysts. A series of gel-type and macroreticular acidic polystyrene-divinylbenzene (PS-DVB)-based ion-exchange resins were used as catalysts to check their performance in hydroxyalkylation/alkylation of 2-methylfuran with butanal. These were Amberlyst15 (A15), Amberlyst16 (A16), Amberlyst35 (A35), Amberlyst39 (A39), Dowex 50Wx2 (D2), Dowex 50Wx4 (D4), and Dowex 50Wx8 (D8). All resins were supplied in wet form and used in the as-received particle size. The mesh size distribution of Dowex resins was 50−100. Resins were first dried and activated for 2 h at 120 °C at 1 atm and then overnight under a vacuum at 100 °C and 0.1 mbar. The final water content after drying was 3−4 wt % (Karl Fischer titration).

2.3. Apparatus and Analytical Methods. The experimental setup consisted of a 200 mL stainless steel stirred tank batch reactor equipped with a six-blade magnetic stirrer (Autoclave Engineers; PA, USA). The working temperature range was 50−90 °C, controlled within ±0.1 °C by means of a thermostatic bath filled with a 50 vol % mixture of propylene glycol and water. The reactor pressure was maintained at 1.5 MPa with nitrogen to widely exceed the vapor pressure of the reaction mixture at the highest assayed temperature to ensure that the reaction was performed in the liquid phase and to impel samples from the reactor to the gas chromatograph.

The reaction mixture was analyzed by injecting online samples of 0.2 μL of pressurized liquid in a gas chromatograph (Agilent 6890, US) equipped with a capillary column HP PONA 19091S-001 (5% phenyl methyl siloxane 50.0 m × 0.2 mm × 0.5 μm nominal) and a mass spectrometer detector (Agilent 5973N, US). A second gas chromatograph (Hewlett-Packard GC 6890A), equipped with a TCD detector, was used to measure the water content by injecting liquid samples of 0.2 μL, taken from the reactor after finishing the experiment, and using a 50 m × 0.2 mm × 0.5 μm methyl silicone HP 90915−001 capillary column. The temperature program consisted of a 6 min initial hold at 45 °C, followed by a 30 °C min^{-1} ramp up to 180 °C, held for 5 min. A total flow rate of 30 mL min^{-1} of a carrier gas (He) was used.

2.4. Procedure and Calculations. In the screening, a molar stoichiometric ratio R_0 (2MF/butanal) = 2 was used, corresponding to a 53.28 g of butanal and 121.54 g of sylvan. A catalyst load of 1 wt % was introduced by a pressure drop when the working temperature of 50 °C had been reached. After that, the reactor was pressurized to 1.5 MPa; that moment was considered as the starting reaction time. The typical total duration of the experiments was 5.4 h. A stirring rate of 750 rpm was considered high enough to avoid the possible influence of external mass transfer. However, some effect of the internal mass transfer is expected since resins were used in commercial particle sizes. This fact has no transcendence in the reported results, as the main screening goal was to compare the catalytic behavior of a series of resins from an industrial application standpoint rather than rigorous kinetic modeling. The effect of the catalyst load (1 and 2 wt %) was also studied by two additional experiments, 8 h in length, under identical experimental conditions. The effect of the reaction temperature was studied within 50−90 °C using 1 wt % of the catalyst load. In addition, the resin stability during three reaction cycles was checked for the most promising catalyst. After a typical run, the used resin was filtered and stirred overnight in 50 mL of 30 vol % H_2O_2 for its regeneration. After another filtration, the catalyst was washed with deionized water (30 mL × 3) and methanol (30 mL × 1). Finally, the recovered resin was dried overnight at 100 °C before reuse.

For each experiment, butanal conversion and yield to BSB were calculated by eqs 1 and 2, respectively. As no butanal-derived byproducts were detected, the butanal selectivity to BSB was always 100% (at 50 °C), and thus, the butanal conversion and yield of BSB were equivalent.

$$X_{\text{butanal}} = \frac{\{\text{mole of reacted butanal}\}}{\{\text{initial mole of butanal}\}} = \frac{n^0_{\text{butanal}} - n_{\text{butanal}}}{n^0_{\text{butanal}}} \quad (1)$$

$$Y^{\text{BSB}}_{\text{butanal}} = X_{\text{butanal}} S^{\text{BSB}}_{\text{butanal}} = \frac{\{\text{mole of reacted butanal to BSB}\}}{\{\text{initial mole of butanal}\}} = \frac{n_{\text{BSB}}}{n^0_{\text{butanal}}} \quad (2)$$

To account for the slight variations in the weighed catalyst mass (W_{cat}), the reaction time was standardized in terms of contact time (eq 3) for a suitable comparison among catalysts.

$$\text{contact time} = \frac{tW_{\text{cat}}}{n^0_{\text{butanal}}} \quad (3)$$

After evaluating different mathematical expressions to be used as an empirical model, a reciprocal quadratic function of the form $y = x/(a + bx + cx^2)$ was used to fit to the BSB mole evolutions. Subsequently, the formation rates (r_{BSB}) at any time (t) were estimated as

$$r_{\text{BSB}} = \frac{1}{W_{\text{cat}}}\left[\frac{dn_{\text{BSB}}}{dt}\right]_t \quad (4)$$

where W_{cat} is the dry catalyst mass and n_{BSB} is the BSB mole. Initial reaction rates (r^0_{BSB}) were calculated at the initial instant, and the catalysts turnover frequencies (TOF) [mol h^{-1}

https://dx.doi.org/10.1021/acs.iecr.0c04308
Ind. Eng. Chem. Res. XXXX, XXX, XXX−XXX

eq^{-1}] were estimated as the quotient of r_{BSB} to the corresponding acid capacity at the instant considered. For all screening experiments, the mass balance was fulfilled within ±5% on a mole basis.

3. RESULTS AND DISCUSSION

f1 **3.1. Catalyst Load and Screening Studies.** Figure 1 presents the normalized reactants and BSB mole evolution for

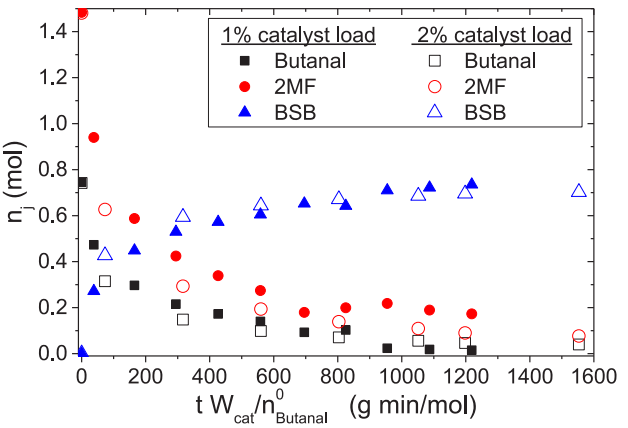

Figure 1. Effect of catalyst load (D2). T = 50 °C, 1.5 MPa, 750 rpm, R_0 (2MF/butanal) = 2, t = 8 h. Hollow symbols refer to a 2% wt catalyst load and filled ones to a 1% wt.

the different catalyst loads evaluated using Dowex 50Wx2 (D2). As expected, the consumption of the reactants was accompanied by an increase of product formed with a consistent fulfillment of the mass balance. Within the experimental error, the molar ratio between reactants was maintained during their consumption throughout the experiment. Noteworthy, the virtually steady composition after 6 h was near chemical equilibrium, suggesting a high reaction equilibrium constant because the BSB formed mole coincides with the initially loaded butanal, in agreement with the reaction stoichiometry. The acceptable overlapping of the corresponding series reveals a negligible effect of the catalyst load. Hereinafter, a loading of 1 wt % will be used for the rest of the runs.

Bearing in mind the physicochemical nature of resins is essential for understanding their catalytic behavior and for a rational interpretation of results. Acidic resins are styrene−divinylbenzene copolymers, in which sulfonic groups are linked to the benzene ring of styrene as active sites. In a conventionally sulfonated resin, the structure holds a maximum of one sulfonic group per styrene ring,[27] whereas, for an oversulfonated resin, such proportion is higher than unity.[28] Gel-type resins are typically translucent beads of homogeneous microstructures without discontinuities. The matrix of such kind of resins is obtained by polymerization in the absence of a solvent called "porogen", and therefore, they do not have permanent pores in a dry state. In this impervious structure, the polymeric matrix is collapsed and renders an almost inactive catalyst after sulfonation because only a few acid centers over the beads external surface are accessible. Conversely, macroreticular resins are opaque beads obtained in the presence of a porogen whose elimination produces a macroporous structure. The resulting net of pores is permanent regardless of the polymer matrix swelling, even at nil swelling conditions in a dry state.[29,30] In short, the catalytic activity of resin will depend strongly on the accessibility to active sites, which, in turn, is dependent on the bulk properties of the resin's working environment.

Gel-type resins primarily exhibit catalytic activity in a medium capable of expanding the polymeric matrix, i.e., when the solubility parameter of the medium (typically in polar solvents, reactants, or products) is similar to that of the resins. On the other hand, macroreticular resins exhibit catalytic activity in both swelling and nonswelling conditions due to their permanent porosity.[27,31,32] As an illustrative representation, Figure 2 shows the three types of pores found in a

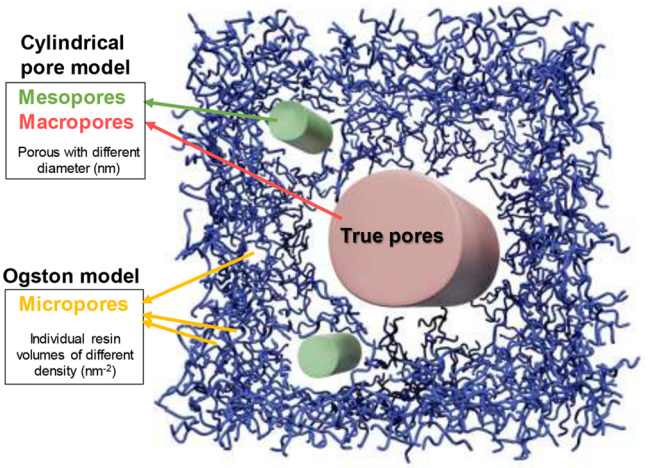

Figure 2. Schematic representation of the types of pores in swollen macroreticular resins and linking to the models applied for their description.

macroreticular resin in a swollen state: (i) micropores of the nonswelling inaccessible part of the polymeric matrix, (ii) new mesopores formed by swelling, and (iii) macropores from the permanent porosity. However, gel-type resins in the swollen state contain only two types of pores (i and ii), which gradually vanish during shrinking. The extension of the microporous and mesoporous zones depends on the swelling degree. In highly polar mediums, such as water, the resin will be very swollen, showing accessibility to practically all active sites. The inaccessible zone of micropores is negligible, and the entire polymer matrix presents a mesoporous structure. Accordingly, the resin's morphological properties are dynamic and depend on the reaction medium polarity, which often varies with the course of the reaction. The understanding of such a complex scenario is paramount to interpret the results comprehensively. For instance, it can be useful to link the catalytic behavior to the resin properties of the resin in a dry state for nonpolar conditions, whereas it is more reasonable to link the behavior of the resin to properties obtained in a swollen state for polar reaction mediums. Consequently, approaches based on porosimetric information (nitrogen adsorption/desorption and mercury porosimetry) are more appropriate to understand resin performance in nonpolar conditions, but they become unsuitable for explaining the behavior under swelling in the presence of polar solvents.

Inverse steric exclusion chromatography (ISEC)[33] is a useful characterization technique for describing the resin morphology in a swollen state. In the fundamentals of that method, macroporous and mesoporous regions are simulated by the cylindrical pore model, while microporous zones are simulated

https://dx.doi.org/10.1021/acs.iecr.0c04308
Ind. Eng. Chem. Res. XXXX, XXX, XXX−XXX

Table 1. Characteristics and Structural Parameters of Resins in the Dry State and Swollen in Water

						dry state[d]		swollen in water[g]		
type[a]	catalyst	sulfonation type[b]	T_{max} (°C)	$[H^+]$[c] (mmol/g)	DVB (%)	S_g[e] (m^2/g)	V_g[f] (cm^3/g)	S_g (m^2/g)	V_{sp} (cm^3/g)	$[H^+]/V_{sp}$ (mmol/cm^3)
M	A35	OS	150	5.32	20	34	0.21	199	0.50	10.6
M	A15	CS	120	4.81	20	42	0.33	192	0.62	7.8
M	A16	CS	120	4.80	12	1.7	0.013	46	1.14	4.2
M	A39	CS	130	4.81	7−8	0.09	3×10^{-4}	56	1.64	2.9
G	D8	CS	150	4.80	8	0	0	0	1.40	3.4
G	D4	CS	150	4.95	4	0.011	0	0	1.90	2.6
G	D2	CS	150	4.98	2	0	0	0	2.68	1.9

[a]Macroreticular (M) and gel (G). [b]Conventionally sulfonated (CS) and oversulfonated (OS). [c]Acid capacity. Titration against a standard base. [d]By adsorption−desorption of N_2 at 77 K (N_2 for $S_g \geq 1$ m^2/g; Kr for $S_g < 1$ m^2/g). [e]BET method. [f]Volume of N_2 adsorbed at a relative pressure $P/P_0 = 0.99$. [g]ISEC (Inverse steric exclusion chromatography) method.

by the geometrical model proposed by Ogston,[34] in which micropores are described as spaces between randomly oriented rigid rods, representing the polymer chains. The main characteristic parameter from ISEC is the specific volume of the swollen polymer, V_{sp}, in cm^3/g, which includes the volume of the free space plus that occupied by the skeleton. Table 1 shows the V_{sp} of the tested resins, textural properties determined in a swollen and dry state, and some other relevant physicochemical properties. T_{max} is the maximum temperature for thermal stability, $[H^+]$ is the acid capacity, DVB is the percentage of the cross-linking agent, S_g is the specific surface area, V_g is the volume of pores on the dry state, and $[H^+]/V_{sp}$ is the acid density of the swollen polymer. As it can be seen, V_{sp} decreases as DVB increases both for gel-type and macroreticular resins. Low V_{sp} values imply a high density of polymer matrix in the swollen state and, as a result, poorly accessible spaces even for small molecules. Conversely, high V_{sp} values are associated with a low density of polymer mass and large spaces, which can be accessible for even large molecules.

Figure 3 plots the evolution of the butanal conversion for Dowex gel-type resins. At the end of the runs, $X_{butanal}$ was

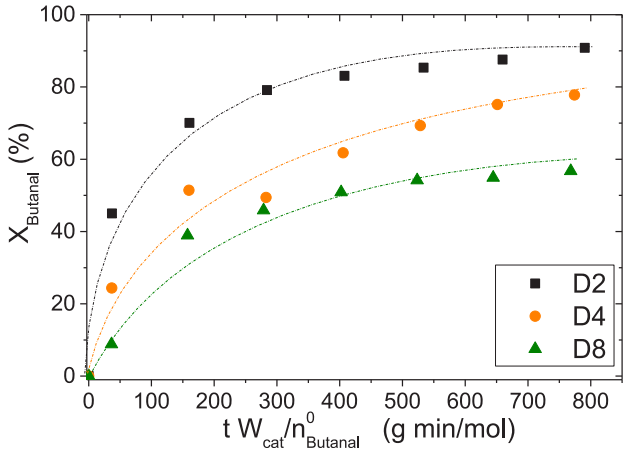

Figure 3. Butanal conversion versus contact time for gel-type resins. T = 50 °C, 1.5 MPa, R_0 (2MF/butanal) = 2, catalyst loading 1 wt %, t = 5.4 h. Dashed lines are a guide to the eye.

about 90% for the resin D2, which has the lowest cross-linking degree, followed by 80% for D4 and about 60% for D8. Among them, D2 was the most active gel-type resin reflected in the steepest curve, indicating a faster reaction rate. As the acid capacity of these resins increases, so does the reported conversions. However, that difference (e.g., between D4 and D2 resins: 4.98 and 4.95 mmol/g) does not justify the significantly different activity observed. This suggests that accessibility, and thus swelling, plays a paramount role in the catalytic activity, which can be explained on the basis of the morphology of such type of resins; they progressively swell as the reacting medium becomes more polar, mainly induced by the presence of formed water, enhancing, therefore, accessibility to active sites with the course of the reaction. As the resins cross-linking degree decreases (D8 > D4 > D2), the swelling capacity or V_{sp} increases (see Table 1), leading to an increase in the flexibility of polymer chains and, hence, to improved accessibility to acid sites.

Figure 4 shows the butanal conversion standardized evolution for the different macroreticular resins studied. The

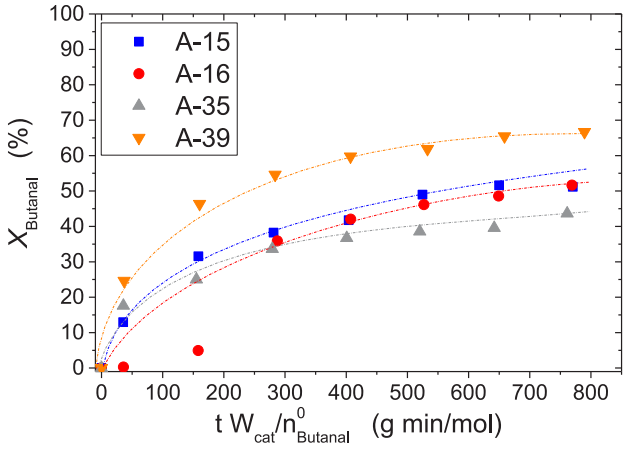

Figure 4. Butanal conversion versus contact time for macroreticular resins. T = 50 °C, 1.5 MPa, R_0 (2MF/butanal) = 2, catalyst loading 1 wt %, t = 5.4 h. Dashed lines are a guide to the eye.

final achieved conversions follow the order A39 > A15 ≈ A16 > A35, which again is consistent with the decreasing order of V_{sp} from Table 1. This fact clearly shows the significant effect of the resin morphology on catalytic behavior. For the resin A16, the experimental data at about 40 and 160 g/(min mol) suggest a sort of induction period. Apart from the inherent experimental uncertainty, this unexpected behavior could be attributed to the lower % DVB of this resin compared to A15 and A35. This results in A16 having a higher ability to swell than A15 and A35; however, its macroreticular and still stiff structure somewhat offers resistance to swelling if compared to D2, D4, and D8 catalysts. Noteworthy, the run using A16 was

https://dx.doi.org/10.1021/acs.iecr.0c04308
Ind. Eng. Chem. Res. XXXX, XXX, XXX−XXX

replicated, and the results confirmed that such behavior was reproducible. As deducted from Figure 3 results, the highest conversion values at the end of the runs were obtained for A39, a resin with a high V_{sp} and low cross-linking degree, which, as mentioned, encompass lower density of polymer chains, larger flexibility, and wider spaces due to their higher ability to swell. Such type of structure enhances the accessibility of reactants to acid sites as well as the diffusion of big-sized product molecules as BSB from those active sites. This relation applies for both gel-type and macroreticular resins, yet under identical experimental conditions, the activity of macroreticular resins is clearly lower than gel-type resins due to the higher % DVB.

Considering the implicit relationship between the concentration of active sites and catalytic activity, the acid capacity must also be taken into account to assess the final conversion and yield reported values. For this purpose, the final yield toward BSB (target product) can be related to the acid density of swollen polymer $[H^+]/V_{sp}$, which is evidently higher for those resins of oversulfonated nature and present a high cross-linking degree. Figure 5 shows a clear relationship between

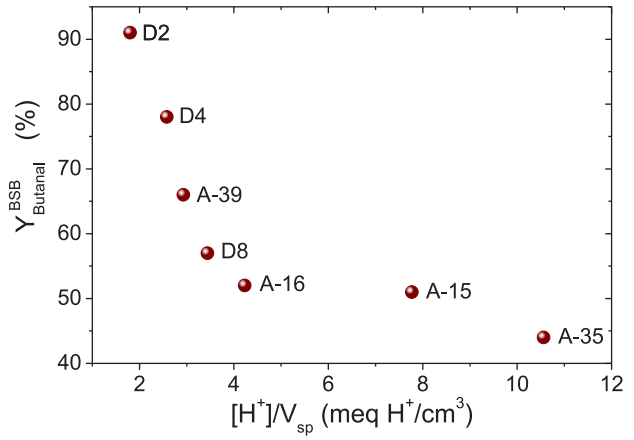

Figure 5. Yield of butanal to BSB, $Y^{BSB}_{butanal}$, versus acid density for macroreticular and gel-type resins. T = 50 °C, 1.5 MPa, R_0 (2MF/butanal) = 2, catalyst loading 1 wt %, t = 5.4 h.

both variables: the final product yield increases with decreasing acid density of the resins. Interestingly, the relation seems to have two clear linear periods: the steepest one including the resins D2, D4, D8, and A39 (with the lowest cross-linking degree) and the less steep period including the macroreticular resins A15, A16, and A35. In comparison with A35, which has the same degree of cross-linking, A15 gives not only a higher butanal conversion and yield but also an apparently faster reaction rate at contact times above 300 (g min)/mol as can be inferred from the steeper slope in Figure 4. This can be explained by the higher pore volume and V_{sp} of A15 that facilitates the internal diffusion of reactants and formed products.

Of course, it is to be noted that resin characterization by ISEC is at swelling conditions in water, and that is not exactly the actual state of the resins in the reaction medium. The initial reaction medium is essentially formed by sylvan and butanal; water was formed as a byproduct with the course of the reaction. Therefore, it could be expected that the resins were not swelled in the initial reaction steps. However, it is to be noted that butanal is also a polar substance, e.g., dipole moment even higher than that of water, and therefore, swelling is expected to occur from the initial steps of the reaction. In this sense, the characterization by ISEC is a reasonable approximation to the morphology of the actual catalysts in reaction conditions, which allows for explaining the catalytic behavior observed for the different catalysts.

In order to assess the initial catalytic activity of the resins evaluated, Figure 6 plots the evolution of the turnover

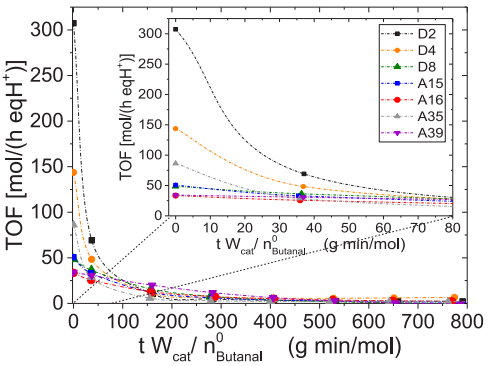

Figure 6. Evolution of turnover frequencies over the resins evaluated vs contact time. T = 50 °C, 1.5 MPa, R_0 (2MF/butanal) = 2, catalyst loading: 1 wt %. The magnification inside highlights the TOF variation at initial contact times.

frequencies with the normalized course of the reaction. As indicative figures, the estimated initial BSB formation rates for the resins D2, D4, D8, A35, A15, A16, and A39 were 1530.8, 711.3, 233.7, 458.79, 243.6, 160.4, and 628.74 mol/(h kg_{cat}), respectively. These values confirm one of the original motivations of the present work, demonstrating that gel-type resins are more efficient catalysts, in terms of yield to target products, product formation rates, and TOF, for reactions involving the formation of water than their macroreticular analogous. Interestingly, the initial TOF for A35 was surprisingly high, even higher than those of D8 and A15 resins. An explanation to this fact may arise from the highest acid density ($[H^+]/V_{sp}$) of this resin that confers a very high initial catalytic activity. However, as the reaction proceeds and products are formed, the diffusional limitations derived from the resistance to swelling play a notable detrimental role in the activity. The immediate aftermath of the oversulfonation, e.g., in A35, is a stiffer structure between polymer chains of the resins because there are more sulfonic groups prone to hydrogen bond the involved chemical species confined in the same space. This leads to reduced accessibility to acid centers and, eventually, to a lower product yield. In this case and as the reaction proceeds, the greater acid capacity of A35 does not make up for its major rigidity, which plays a more prominent role in the catalytic behavior observed.

In spite of the similar acid capacity of A16, A15 exhibits a greater surface area (S_g) in the swollen state (Table 1), which leads to a better macropore diffusion toward the gel phase and an improved initial catalytic activity (Figure 6). On the other hand, A16 has an almost double-fold volume of the gel phase (V_{sp}). In other words, a better micropore diffusion of molecules inside the gel phase of A16, yet the access to this gel phase by previous macropore diffusion is more hindered. The balance between these two opposite effects opts slightly for the better permeation, i.e., micropore diffusion, inside the gel phase of A16. As a result, A16 gains activity with the course

https://dx.doi.org/10.1021/acs.iecr.0c04308
Ind. Eng. Chem. Res. XXXX, XXX, XXX−XXX

Table 2. Compendium of Reported Values of Butanal Conversion and BSB Selectivity and Yield for the HAA of Sylvan with Butanal over Different Catalysts

entry	catalyst	T (°C)	R_0 (2MF/butanal)	W_{cat} (%)	t (h)	$X_{butanal}$ (%)	$Y^{BSB}_{butanal}$ (%)	$S^{BSB}_{butanal}$ (%)	ref
1	$NbOPO_4$	80	2.05	4	5	95.3	89.5		18
2	IGO	60	2	2.9	6		83		19
3	copper triflate	room	2	10[a]	8		58		20
4	Sn-β(12.5) zeolite	100	2	2	10		81		21
5	Nafion 212	50	2	3	2	96.7[b]	88.4[b]		22
6	Nafion 212	50	2	3	4	91	81	89	15
7	60LS4OPS35OH$^+$Na-lignosulfonate derived acidic carbocatalyst	60	2	3	2	99	96		24
8	KCC-1APSO$_3$H	50	2	3	4	100	94	94	15
9	protonated titanate nanotubes	50	2	3	4	70[b]	68[b]		23
10	A15	50	2	3	4	64	47	73	15
11	A15	50	2	3	2	80[b]	72[b]		22
12	A15	50	2	2.3	22	72	59	82	12
13	A15	50	3	1.7	22	80	69	86	12
14	A15	50	2	1.2	8		90[c]		8
15	A15	50	2	1	5.4	51	51	100	this work
16	A36	50	2	3	2	72[b]	70[b]		22
17	A36	50	2	3	4	66	50	75	15
18	D2	50	2	1.2	8		80[c]		8
19	D2	50	2	1	5.4	90	90	100	this work

[a]Based on mol %. [b]Values referred to 2MF conversion, and therefore, selectivity and yield values are referred to the production of BSB from 2MF. [c]Yield of 2,2′-butylidenebis[5-methylfuran] with a purity of at least 93% after 8 h reaction time.

of the reaction, reaching final BSB yields comparable to those obtained with A15 that exhibited higher initial activity.

The resin A39 has a similar acid capacity to those of A15 and A16, but it is the resin with the lowest cross-linking degree and, therefore, the more flexible structure among the macroreticular resins studied. In the swollen state, A39 exhibits comparable surface area to that of A16 and smaller than A15. However, the swollen state pore volume of A39 significantly exceeds those of A15 and A16, owing to its lower cross-linking degree. As a result, its initial level of activity is comparable to that of the gel-type resin D4 (Figure 6). As the reaction medium becomes more polar by the formation of water, this is translated into an enhanced catalytic activity that increases with the course of the reaction. This can also be clearly seen in the steeper slope between 0 and 400 (g min)/mol in Figure 4, which eventually leads to the high BSB yield reported for this resin at the end of the runs.

Aiming to provide a general overview of the current state of the art framework exposed in the introduction and the results reported in this work, Table 2 gathers a collection of butanal conversion, BSB selectivity, and reported yield values for comparison. In some cases, the butanal conversion and its yield toward BSB are equivalent because neither the literature data nor this work detected the presence of butanal-derived byproducts. The HAA of sylvan with butanal over $NbOPO_4$ at 80 °C resulted in 95.3% of butanal conversion and 89.5% of BSB yield after 5 h.[18] The BSB yield of 83% was obtained at 60 °C using a molar ratio of sylvan to butanal R_0 (2MF/butanal) = 2 after 6 h of reaction over improved graphene oxide (2.9 wt % loading).[19] Using copper(II) triflate under solvent-free conditions,[20] a 58% BSB yield was obtained after 8 h of reaction at room temperature, and the catalyst withstood four successive cycles without significant deactivation. In another approach,[21] for the alkylation step at 100 °C with a 2MF/butanal molar ratio of 2 and a catalyst loading of 2 wt %, Sn-beta (12.5) zeolite exhibited the best catalytic performance, yielding 81% of the corresponding alkylated product after 10 h. The catalyst was fully recyclable in an aqueous solution with constant product selectivity (70−72%) after six successive runs. However, both 2MF conversion and the corresponding product yield decreased slightly in the last cycle, which was ascribed to the deposition of organic species into zeolite pores.

Li et al. (2013)[22] reported high 2MF conversion (96.7%) and BSB selectivity (88.4%) at 50 °C using a 2MF/butanal molar ratio of 2 and a catalyst (Nafion 212) loading of 3 wt % after 2 h. In that study, 2MF conversion for Amberlyst15 (A15) and Amberlyst36 (A36) were 81% and 72%, respectively, with high BSB selectivities (>90%) without evidence of 2MF trimer formation. It was concluded that Nafion and Amberlyst sulfonic groups can catalyze the reaction, while H-ZSM-5, H-USY, and H-β zeolites are practically inactive due to their smaller pore diameter by considering the size of the BSB molecule. The results were consistent with those reported by Wen et al. (2014),[3] revealing that zeolite type catalysts are mainly suitable candidates for the HDO step, which must be performed at considerably higher temperatures (200−400 °C). In terms of stability, Nafion 212 and A15 were remarkably stable for the HAA of 2MF with butanal after 5 cycles, but A36 exhibited slight deactivation.[22] In addition, the activity of the catalysts tested was consistent with their acid strength. In a different attempt at 50 °C using the same molar ratio and a 0.15 g of the protonated titanate nanotube as the catalyst,[23] high 2MF conversion (~70%) and selectivity were reported after 4 h of reaction. However, the catalysts deactivated slightly after 3 cycles at the same experimental conditions. In another study, 72% of butanal conversion with 82% BSB selectivity was obtained over A15 (2.5 wt %) at 50 °C using a molar ratio of 2MF/butanal of 2 after 22 h.[8] At identical reaction conditions but a lower catalyst load (1.15 wt %) and shorter reaction time (8 h), the same authors reported striking BSB yield values of 90% and 80% for A15 and Dowex 50Wx2, respectively.[12]

https://dx.doi.org/10.1021/acs.iecr.0c04308
Ind. Eng. Chem. Res. XXXX, XXX, XXX−XXX

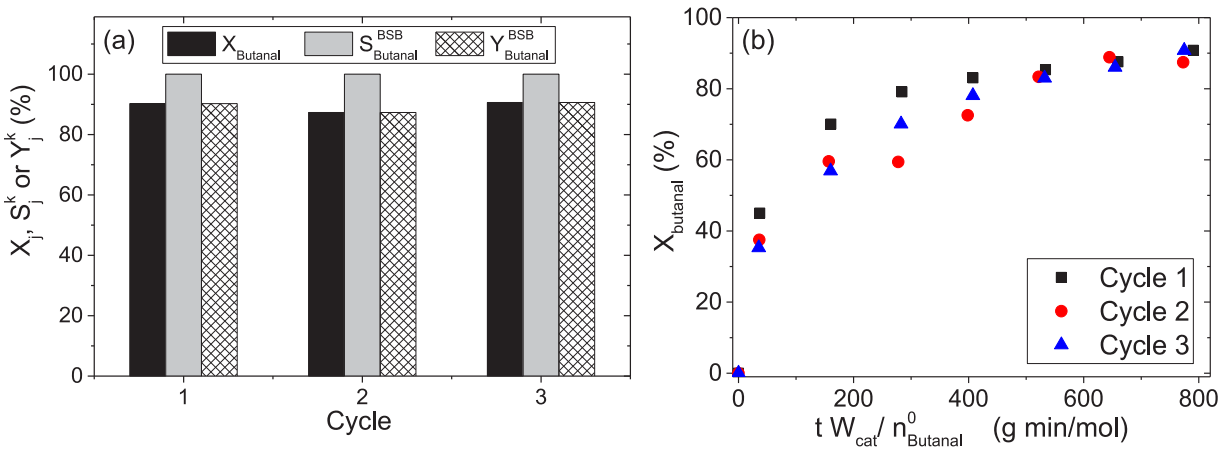

Figure 7. (a) Butanal conversion, selectivity, and yield in each cycle at t = 5.4 h. (b) Evolution of butanal conversion for each cycle. Experimental conditions: 1.5 MPa, 750 rpm, molar ratio R_0 (2MF/butanal) = 2, catalyst loading 1 wt % (D2).

Using sulfonic acid-based catalysts supported on silica nanoparticles for this reaction at 50 °C, R_0 (2MF/butanal) = 2, catalyst loading of 3 wt %, and reaction time of 4 h,[15] KCC-1APSO$_3$H catalysts exhibited the highest conversion (100%) and BSB selectivity (94%), followed by Nafion 212 (91% conversion and 89% selectivity). High butanal conversions of 64% and 66% and selectivities to BSB of 73% and 75% were respectively reported over A15 and A36. Na-lignosulfonate (LS)-derived meso/macroporous solid sulfonic carbocatalysts in the solvent-free HAA of 2MF with butanal, 60LS40PS350H$^+$ exhibited an outstanding carbonyl conversion of 99% and BSB yield of 96% along with minimal deactivation (only 2% in terms of conversion) after three reaction cycles.

The comparison between the literature values in Table 2 is not always straightforward because of the different experimental conditions, e.g., catalyst load, reaction temperature, reaction times, or the basis of reported values. However, the butanal conversion follows the expected trend: it increases with an increasing molar ratio of 2MF to butanal, catalyst load, and reaction time. In general, our reported values for A-15 compare acceptably well with those obtained by Gebresillase et al.[15] and Corma et al.[12] under similar conditions. However, a significant discrepancy is observed in comparison to Table 2, entry 14, which can be explained by the longer reaction time of 8 h used in that study. Interestingly, the studies using catalyst loads above 1.2 wt % report butanal selectivity to BSB values lower than 100% irrespectively of the 2MF/Butanal molar ratio used. Noteworthy, our experiments with 1 wt % of A-15 were replicated, and butanal-derived byproducts were never detected at 50 °C. This highlights the importance of an optimum catalyst load to avoid side reactions. Conversely, butanal conversion values for D2 resin are more comparable because of more similar experimental conditions. Our values are reasonably similar to those reported by Corma et al.[8] However, a more rigorous comparison would require to consider the catalyst particle size used in the reference experiment (Table 2, entry 18) since commercial D2 can be supplied in different mesh sizes (50−100, 100−200, and 200−400). An overall outcome emerging from the comparison in Table 2 is that D2 presents a catalytic activity comparable to that reported for the best catalysts previously studied (60LS4OPS35OH$^+$Na$^-$-lignosulfonate-derived acidic carbocatalyst, KCC-1APSO$_3$H, NbOPO$_4$, and Nafion 212), taking into account the different catalyst loads and reaction times reported. This fact, along with the appealing features of ion-exchange resins in terms of cost, pinpoints D2 as a potential catalyst for the production of BSB by the HAA of 2MF with butanal.

3.2. Effect of Temperature. As mentioned, no significant byproducts derived from sylvan were detected at 50 °C, molar R_0 (2MF/butanal) = 2, 1 wt % catalyst loading of D2, and t = 5.4 h. However, at 60 °C, byproducts began to appear (3% GC), representing their presence of 10% GC at 70 °C and 23% GC at 90 °C. In agreement with the literature,[9,14,15,21] the main byproduct detected, of higher molar mass than BSB, was the 2MF trimer (5,5-bisylvyl-2-pentanone). Unfortunately, the rest of the byproducts could not be properly identified by MS due to their low amount. The reaction pathway for the generation of BSB and oligomers of sylvan is illustrated in Schemes 1 and 2, respectively. Even though both butanal and 2MF conversion increase with temperature, a significant decrease in the 2MF selectivity to BSB eventually leads to an important depletion of the BSB yield. Thus, it can be concluded that, to minimize byproducts formation, temperatures below 60 °C, R_0 (2MF/butanal) = 2, and 1 wt % of catalyst load are the most appropriate conditions for conducting the HAA reaction between sylvan and butanal catalyzed by the acidic ion-exchange resin D2.

3.3. Reusability. As the most promising catalyst, D2 was reused three times by following the previously detailed reactivation procedure. Figure 7a shows conversion, selectivity, and yield obtained at the end of the runs in each cycle. The butanal selectivity to BSB (100%) remained unchanged after three cycles. Butanal conversion, however, decreased slightly (less than 3%), which can be considered negligible, taking into account the experimental uncertainty. Under similar experimental conditions,[22] no deactivation was detected over A15 after five cycles, basing the calculations on the 2MF conversion and yield as a reference. For a better assessment of the catalyst stability, Figure 7b depicts the evolution of butanal conversion in each cycle. Noteworthy, some signs of loss of initial catalytic activity (~10%) were observed at the beginning of the runs, yet identical conversion values were reported for contact times of 500 (g min)/mol onward. Although the performance of the most promising catalyst evaluated in this work must still be evaluated in different practical scenarios, particularly in flow conditions with long times on stream for its industrial application, the results herein reported reveal a positive and

https://dx.doi.org/10.1021/acs.iecr.0c04308
Ind. Eng. Chem. Res. XXXX, XXX, XXX−XXX

favorable insight for considering D2 resin as a potential catalyst with high activity, selectivity, and stability, for the HAA reaction of 2MF with butanal.

4. CONCLUSIONS

The catalytic hydroxyalkylation/alkylation of 2-methylfuran with butanal at a stoichiometric molar ratio can be successfully catalyzed by ion-exchange resins at the temperature range 50−90 °C. Butanal conversion increases with temperature but so does the formation of 2-methylfuran oligomers, leading to an overall decrease of yield to BSB. The catalytic activity and yield to the target product of gel-type resins are superior to those of macroreticular ones due to their ability to swell during the reaction by the formation of water, which promotes enhanced accessibility to active sites. Among the resins evaluated, the most promising catalyst (Dowex 50Wx2) presents the lowest cross-linking degree and achieves notably high butanal conversion (90%) and selectivity to BSB (100%) at 50 °C, without significant formation of 2-methylfuran oligomers. Macroreticular resins with low content of a cross-linking agent also give acceptable catalytic behavior. The catalytic activity rank observed in terms of final yield to target product can be rationalized on the basis of the resin morphological properties: the activity increase with decreasing acid density, i.e., the ratio of acid capacity to the volume of the swollen polymer. This fact highlights the paramount importance of enhanced accessibility to improve diffusivity for the present reaction system that involves products of significant molecular volume. The reusability of the most prominent catalyst (D2) has been evaluated after three reaction cycles, and the results suggest that it is a stable catalyst with the industrial prospective application for the studied reaction system.

AUTHOR INFORMATION

Corresponding Author

Eliana Ramírez − *Department of Chemical Engineering and Analytical Chemistry, Faculty of Chemistry, University of Barcelona, 08028 Barcelona, Spain;* orcid.org/0000-0001-8695-1533; Email: eliana.ramirez-rangel@ub.edu

Authors

Rodrigo Soto − *Synthesis and Solid State Pharmaceutical Centre (SSPC), Bernal Institute, Department of Chemical and Environmental Science, University of Limerick, Limerick V94 T9PX, Ireland;* orcid.org/0000-0002-9988-7494

Roger Bringué − *Department of Chemical Engineering and Analytical Chemistry, Faculty of Chemistry, University of Barcelona, 08028 Barcelona, Spain*

Montserrat Iborra − *Department of Chemical Engineering and Analytical Chemistry, Faculty of Chemistry, University of Barcelona, 08028 Barcelona, Spain*

Javier Tejero − *Department of Chemical Engineering and Analytical Chemistry, Faculty of Chemistry, University of Barcelona, 08028 Barcelona, Spain;* orcid.org/0000-0002-2708-5273

Complete contact information is available at: https://pubs.acs.org/10.1021/acs.iecr.0c04308

Notes

The authors declare no competing financial interest.

ACKNOWLEDGMENTS

The authors are grateful to MINECO (CTQ2014-56618-R Grant) for their financial support and Rohm and Haas France S.A.S for providing ion-exchange resins samples. Also, we thank Laura González Saladich for the help with the graphic design of the artwork.

NOTATION

ABE = acetone-butanol-ethanol
A15 = Amberlyst15
A16 = Amberlyst16
A35 = Amberlyst35
A39 = Amberlyst39
BSB = 1,1-bysylvylbutane
DVB = divinyl benzene
D2 = Dowex 50Wx2
D4 = Dowex 50Wx4
D8 = Dowex 50Wx8
GC = gas chromatography
HAA = hydroxyalkylation/alkylation
HDO = hydrodeoxygenation
$[H^+]$ = acid capacity, mmol/g
$[H^+]/V_{sp}$ = acid site density in swollen resins, mmol/cm^3
IGO = improved graphene oxide
(LS) = Na-lignosulfonate
$n^0_{butanal}$ = initial mole of butanal
$n_{butanal}$ = mole of butanal
n_{BSB} = mole of BSB
PS-DVB = polystyrene-divinylbenzene-based resins
$R_{0(2MF/butanal)}$ = molar ratio of sylvan to butanal
$S^{BSB}_{butanal}$ = selectivity of butanal toward BSB
S_g = specific area, m^2/g
t = time, min
T = temperature, °C
TCD = thermal conductivity detector
T_{max} = maximum temperature of resins for stability, °C
V_g = specific volume of pores, cm^3/g
V_{sp} = swollen specific volume of gel phase, cm^3/g
W_{cat} = dried mass of catalyst, g
$X_{butanal}$ = butanal conversion
$Y^{BSB}_{butanal}$ = yield of butanal toward BSB
2MF = 2-methylfuran

REFERENCES

(1) Garcia-Ortiz, A.; Arias, K. S.; Climent, M. J.; Corma, A.; Iborra, S. Transforming methyl levulinate into biosurfactants and bio-lubricants by chemoselective reductive etherification with fatty alcohols. *ChemSusChem* **2020**, *13*, 707−714.

(2) Climent, M. J.; Corma, A.; Iborra, S. Conversion of biomass platform molecules into fuel additives and liquid hydrocarbon fuels. *Green Chem.* **2014**, *16*, 516−547.

(3) Wen, C.; Barrow, E.; Hattrick-Simpers, J.; Lauterbach, J. One-step production of long-chain hydrocarbons from waste-biomass-derived chemicals using bi-functional heterogeneous catalysts. *Phys. Chem. Chem. Phys.* **2014**, *16*, 3047−3054.

(4) Zainol, M. M.; Amin, N. A. S.; Asmadi, M.; Ramli, N. A. S. Esterification of levulinic acid to ethyl levulinate using liquefied oil palm frond-based carbon cryogel catalyst. *BioEnergy Res.* **2019**, *12*, 359−369.

(5) Hamdi, J.; Diehl, B. N.; Kilgore, K.; Lomenzo, S. A.; Trudell, M. L. Halloysite-catalyzed esterification of bio-Mass derived acids. *ACS Omega* **2019**, *4*, 19437−19441.

(6) Kumar, P.; Varkolu, M.; Mailaram, S.; Kunamalla, A.; Maity, S. K. Biorefinery polyutilization systems: Production of green trans-

https://dx.doi.org/10.1021/acs.iecr.0c04308
Ind. Eng. Chem. Res. XXXX, XXX, XXX−XXX

portation fuels from biomass. In *Polygeneration with Polystorage Chem. Energy Hubs*; Khalilpour, K. R., Ed.; Elsevier: London, 2018; pp 373−407.
(7) Ramírez, E.; Bringué, R.; Fité, C.; Iborra, M.; Tejero, J.; Cunill, F. Role of ion-exchange resins as catalyst in the reaction-network of transformation of biomass into biofuels. *J. Chem. Technol. Biotechnol.* **2017**, *92*, 2775−2786.
(8) Corma, A.; De La Torre, O.; Renz, M. Production of high quality diesel from cellulose and hemicellulose by the Sylvan process: Catalysts and process variables. *Energy Environ. Sci.* **2012**, *5*, 6328−6344.
(9) Gandarias, I.; García-Fernández, S.; Obregón, I.; Agirrezabal-Telleria, I.; Arias, P. L. Production of 2-methylfuran from biomass through an integrated biorefinery approach. *Fuel Process. Technol.* **2018**, *178*, 336−343.
(10) Wang, C.; Xu, H.; Daniel, R.; Ghafourian, A.; Herreros, J. M.; Shuai, S.; Ma, X. Combustion characteristics and emissions of 2-methylfuran compared to 2,5-dimethylfuran, gasoline and ethanol in a DISI engine. *Fuel* **2013**, *103*, 200−211.
(11) Zhang, X.; Deng, Q.; Han, P.; Xu, J.; Pan, L.; Wang, L.; Zou, J.-J. Hydrophobic mesoporous acidic resin for hydroxyalkylation/alkylation of 2-methylfuran and ketone to high-density biofuel. *AIChE J.* **2017**, *63*, 680−688.
(12) Corma, A.; de la Torre, O.; Renz, M.; Villandier, N. Production of high-quality diesel from biomass waste products. *Angew. Chem., Int. Ed.* **2011**, *50*, 2375−2378.
(13) Schlögl, R. *Chemical Energy Storage*; De Gruyter: Berlin, 2013.
(14) Green, S. K. *Production of Renewable Fuels and Chemicals from Biomass-Derived Furan Compounds*. Ph.D.Thesis, University of Massachusetts, November 2014.
(15) Gebresillase, M. N.; Shavi, R.; Seo, J. G. A comprehensive investigation of the condensation of furanic platform molecules to C14-C15 fuel precursors over sulfonic acid functionalized silica supports. *Green Chem.* **2018**, *20*, 5133−5146.
(16) Ishigaki, A.; Shono, T. The cationic oligomerization of 2-Methylfuran and the characteristics of the oligomers. *Bull. Chem. Soc. Jpn.* **1974**, *47*, 1467−1470.
(17) Nakagawa, Y.; Tamura, M.; Tomishige, K. Recent development of production technology of diesel- and jet-fuel-range hydrocarbons from inedible biomass. *Fuel Process. Technol.* **2019**, *193*, 404−422.
(18) Xia, Q.; Xia, Y.; Xi, J.; Liu, X.; Zhang, Y.; Guo, Y.; Wang, Y. Selective One-Pot Production of high-grade diesel-range alkanes from furfural and 2-Methylfuran over Pd/$NbOPO_4$. *ChemSusChem* **2017**, *10*, 747−753.
(19) Dutta, S.; Bohre, A.; Zheng, W.; Jenness, G. R.; Nunez, M.; Saha, B.; Vlachos, D. G. Solventless C-C coupling of low carbon furanics to high carbon fuel precursors using an improved graphene oxide carbocatalyst. *ACS Catal.* **2017**, *7*, 3905−3915.
(20) Muthyala, M. K.; Rao, V. K.; Kumar, A. $Cu(OTf)_2$ Catalyzed synthesis of bis(5-methyl-2-furyl)methanes by condensation of 2-Methylfuran with carbonyl compounds under solvent free conditions. *Chin. J. Chem.* **2011**, *29*, 1483−1488.
(21) Li, H.; Gui, Z.; Yang, S.; Qi, Z.; Saravanamurugan, S.; Riisager, A. Catalytic tandem reaction for the production of jet and diesel fuel range alkanes. *Energy Technol.* **2018**, *6*, 1060−1066.
(22) Li, G.; Li, N.; Yang, J.; Wang, A.; Wang, X.; Cong, Y.; Zhang, T. Synthesis of renewable diesel with the 2-methylfuran, butanal and acetone derived from lignocellulose. *Bioresour. Technol.* **2013**, *134*, 66−72.
(23) Li, S.; Li, N.; Li, G.; Li, L.; Wang, A.; Cong, Y.; Wang, X.; Xu, G.; Zhang, T. Protonated titanate nanotubes as a highly active catalyst for the synthesis of renewable diesel and jet fuel range alkanes. *Appl. Catal., B* **2015**, *170*−*171*, 124−134.
(24) Konwar, L.; J. Samikannu, A.; Mäki-Arvela, P.; Mikkola, J. P. Efficient C-C coupling of bio-based furanics and carbonyl compounds to liquid hydrocarbon precursors over lignosulfonate derived acidic carbocatalysts. *Catal. Sci. Technol.* **2018**, *8*, 2449−2459.
(25) Lachter, E. R.; Rodrigues, J. A.; Teixeira, V. G.; Mendonca, R. H.; Ribeiro, P. S.; Villabona-Estupinan, S. Use of ion-exchange resins in alkylation reactions. *Applications of Ion Exchange Materials in Chemical and Food Industries* **2019**, 35−74.
(26) Guilera, J.; Bringué, R.; Ramírez, E.; Iborra, M.; Tejero, J. Synthesis of ethyl octyl ether from diethyl carbonate and 1-octanol over solid catalysts. A screening study. *Appl. Catal., A* **2012**, *413*−*414*, 21−29.
(27) Corain, B.; Zecca, M.; Jeřábek, K. Catalysis and polymer networks − the role of morphology and molecular accessibility. *J. Mol. Catal. A: Chem.* **2001**, *177*, 3−20.
(28) Tejero, M.A.; Ramirez, E.; Fite, C.; Tejero, J.; Cunill, F. Esterification of levulinic acid with butanol over ion Exchange resins. *Appl. Catal., A* **2016**, *517*, 56−66.
(29) Albright, R. L. Porous polymers as an anchor for catalysis. *React. Polym., Ion Exch., Sorbents* **1986**, *4*, 155−174.
(30) Guyot, A. Synthesis and structure of polymer supports. In *Synthesis and Separations using polymer supports*; Sherrington, D. C., Hodge, P., Eds.; Wiley: Chichester, 1988; pp 15.
(31) Sterchele, S.; Centomo, P.; Zecca, M.; Hanková, L.; Jeřábek, K. Dry- and swollen-state morphology of novel high surface area polymers. *Microporous Mesoporous Mater.* **2014**, *185*, 26−29.
(32) Jeřábek, K. Inverse steric exclusion chromatography as a tool for morphology characterization. In *Strategies in size exclusion chromatography*; Potschka, M., Dubin, P. L., Eds.; American Chemical Society Publications: WA, 1996; pp 211−224.
(33) Jeřábek, K. Determination of pore volume distribution from size exclusion chromatography data. *Anal. Chem.* **1985**, *57*, 1595−1597.
(34) Ogston, A. G. The spaces in a uniform random suspension of fibres. *Trans. Faraday Soc.* **1958**, *54*, 1754−1757.

https://dx.doi.org/10.1021/acs.iecr.0c04308
Ind. Eng. Chem. Res. XXXX, XXX, XXX−XXX